IEEE Access
Multidisciplinary ⋮ Rapid Review ⋮ Open Access Journal

Received February 20, 2020, accepted March 6, 2020, date of publication March 10, 2020, date of current version March 20, 2020.

Digital Object Identifier 10.1109/ACCESS.2020.2979890

Event-Triggered Consensus Control for High-Speed Train With Time-Varying Actuator Fault

WEIPING WANG[1,2,3], JINWEI LE[1,2,3], ZHEN WANG[4,5], XIONG LUO[1,2,3], (Member, IEEE), JÜRGEN KURTHS[6], MANMAN YUAN[1,2,3], AND YOU MA[7]

[1]School of Computer and Communication Engineering, University of Science and Technology Beijing, Beijing 100083, China
[2]Beijing Key Laboratory of Knowledge Engineering for Materials Science, Beijing 100083, China
[3]Institute of Artificial Intelligence, University of Science and Technology Beijing, Beijing 100083, China
[4]Center for Optical Imagery Analysis and Learning, Northwestern Polytechnical University, Xian 710072, China
[5]School of Mechanical Engineering, Northwestern Polytechnical University, Xian 710072, China
[6]Institute of Physics, Humboldt-University Berlin, 10099 Berlin, Germany
[7]National Satellite Meteorological Center, Beijing 100081, China

Corresponding author: Weiping Wang (weipingwangjt@ustb.edu.cn)

This work was supported by the National Industrial Internet Security Public Service Platform, the National Key Research and Development Program of China under Grant 2018YFB0803505, the National Natural Science Foundation of China under Grants 81961138010, U1736117, U1836106 and 61602126, the University of Science and Technology Beijing under Grant FRF-BD-19-012A, and the Technological Innovation Foundation of Shunde Graduate School, USTB, under Grant BK19BF006.

ABSTRACT In this paper, the second-order consensus issue of single high-speed train under event-triggered control is studied. First, the dynamics of single high-speed train (HST) is modeled by a cascade of carriages connected by flexible couplers. Then, we propose a novel event-triggering control strategy that doesn't require continuous communication between carriages, thus can save communication and computing resources effectively. Furthermore, by constructing Lyapunov function, sufficient criteria are obtained to ensure the stability and effectiveness of the system. Besides, all carriages in this high-speed train system exclude Zeno behavior. On this basis, the active fault-tolerant control law of the system and the fault detection accuracy are also discussed when the actuator faults. Some examples are finally given to illustrate the effectiveness of theoretical results.

INDEX TERMS High-speed train, event-triggered control, multi-agent systems, fault detection accuracy.

I. INTRODUCTION

With the increase of global population, the requirements for train transport capacity are also increasing in recent years. High-speed train (HST) is a kind of rail transport relying on automatic train control (ATC) system. In order to improve the transport efficiency of trains, many researchers have conducted in-depth research on the control strategy of HST [1]–[4]. However, many existing articles regard the train composed of multiple carriages as a unit to study the control of multiple trains [3], [4], this kind of control strategies ignores the interaction between adjacent carriages caused by couplers, which may cause some unstable factors in the actual multi-train control. Then, Yang and Sun analyzed the characteristics of couplers between carriages and described them with nonlinear hardening/softening springs model [1]. Based on this model, we can transform the control problem of HST into consensus analysis of multi-agent systems (MASs) by treating each carriage as an agent.

The MAS is a collection of multiple agents that involve distributed sensing, communication, and control. Especially, as the foundation problem of MASs, consensus has attracted many researchers' attention because of its broad application prospects [5]–[7]. However, limited communication bandwidth and controller saturation make large-scale centralized consensus control impractical. To solve this problem, some researchers have conducted research on distributed consistent control [8]–[10]. Under distributed control, each agent only needs to exchange information with its neighbors in the communication topology, thereby reducing the global dependence to some extent.

Although with distributed consensus control, it still assumes that the measurement and control signals accessed by the MAS are continuous and prone to severe delays in

The associate editor coordinating the review of this manuscript and approving it for publication was Jun Shen.

actual control. Naturally, sampling control is applied to the consensus control of multi-agent systems. The most basic sampling control uses periodic sampling [11]. However, when the system is tending towards stability, the periodic sampling still uses the same sampling interval as before, so that causes a lot of unnecessary waste of resources [12].

To solve the above-mentioned problem, event-triggering control is proposed [13], [14]. Under the event-triggering control scheme, the instant of sampling calculation and updating control is determined by the pre-set event triggering condition (ETC), and the control imposed on the agent remains constant between the two triggering instants [15]. This means that the system can change the sampling frequency with the change of its state, thus effectively saves a lot of communication and computing resources while ensure the control performance. In recent years, event triggering schemes have been widely used in the research of complex networks [16], nonlinear systems [17], [18], and uncertain systems [19], [20]. But this control strategy brings the possibility of Zeno behavior. Zeno behavior means the occurrence of infinite events in a finite time, which may make the event-triggered scheme unable to work successfully. Therefore, avoidance of Zeno behavior must be considered in the design process.

Reviewing the researches on consensus control of HST in recent years, authors in [21] studied the problem of distributed continuous consensus control for single high speed train. To reduce the communication burden, authors in [22] studied the fixed-time sampling control method for single high-speed train. There are also articles based on the event-triggered scheme to study the control problem of HST. For example, authors in [4] designed event triggering control strategy for multiple trains, but they ignored the influence of interaction force between trains on control effect. Moreover, considering the huge weight and complex physical connection of the high-speed train model, as well as the factor that the event-triggered control remains unchanged between two trigger times, it is necessary to take the actuator fault into account. As an important content of fault-tolerant control, actuator failure has been studied in uncertain nonlinear systems [23] and event-triggered schemes [24]. Although many works have studied single agent fault diagnosis based on fault detection system [25], [26], few papers have analyzed the influence of detection accuracy of fault detection system on system stability.

Motivated by the previous discussions, in this paper, we propose a distributed event-triggered consensus control strategy for the single second-order high-speed train model, which takes the force between adjacent carriages into account. The main contributions of this paper are summarized as follows:

1) A event-triggered consensus control scheme is designed based on second-order high-speed train model. The event-triggering condition only relates to local measurement errors and the state of neighboring carriages at their last triggering time. Compared with some event-triggered controls that require continuous communication with each agent's neighbors [27]–[29], the control scheme we proposed can further save communication resources.

2) The exclusion of Zeno behavior of all carriages is demonstrated, while many articles about distributed event-triggered ignored it or just one agent's Zeno behavior is proved.

3) Active fault-tolerant control for high-speed train with time-varying actuator fault under event triggering control strategy is carried out, and the fault detection accuracy required to ensure the stability of the system is analyzed.

The rest of this paper is organised as follows: Section 2 states some preliminaries and introduces the model of HST. Section 3 introduces the control schemes we proposed and gives the proof of stability. Some simulation experiments are carried out in Section 4 to exhibit the effectiveness and feasibility of the proposed control methodologies, Section 5 gives our conclusion.

II. PRELIMINARIES

A. COMMUNICATION GRAPHS

Let $G = (V, \varepsilon, A)$ denotes a graph consisting of a finite non-empty vertex set $V = \{1, 2, ..., N\}$, an edge set $\varepsilon \subseteq V \times V$, and a weighted adjacency matrix $A = [a_{ij}] \in \mathbb{R}^{n\times n}$, where a_{ij} is the weight satisfying $a_{ij} = 1$ if (j, i) is the edge of G, and otherwise, $a_{ij} = 0$. Moreover, we assume $a_{ii} = 0$ for all $i \in V$. The set of neighbors of node i in G is denoted as $\mathcal{N}_i = \{j \in V : (j, i) \in \varepsilon\}$. Let the matrix $\mathcal{D} = \operatorname{diag}\left\{d_1', d_2', \ldots, d_N'\right\}$ denotes the degree matrix of digraph G, where $d_i' = \sum_{j=1}^{N} a_{ij}$. Finally, define the Laplacian matrix $\mathcal{L} = [l_{ij}]_{n\times n}$ of digraph G as: $\mathcal{L} = \mathcal{D} - A$.

B. SUPPORTING LEMMAS

Lemma 1 [30]: Let $\bar{\mathcal{L}} = \mathcal{L} + D$, where $\mathcal{L}$ is defined above, and D denotes which node in G can receive the message from the leader, therefore, D is a nonnegative diagonal matrix. then $\bar{\mathcal{L}} > 0$ if and only if at least one node in each connected component of G can receive leader's message.

Lemma 2 [31]: Either of the following conditions:

$$\begin{aligned} &1.\quad M(x) > 0, N(x) - P(x)^T M^{-1}(x) P(x) > 0, \\ &2.\quad N(x) > 0, M(x) - P(x) N^{-1}(x) P(x)^T > 0. \end{aligned} \tag{1}$$

is equivalent to the LMI as follow:

$$\begin{bmatrix} M(x) & P(x) \\ P^T(x) & N(x) \end{bmatrix} > 0. \tag{2}$$

Lemma 3: When condition $\forall \psi, \omega \in R$ and $\epsilon > 0$ is satisfied, the following property holds:

$$\psi\omega \le \frac{\epsilon}{2}\psi^2 + \frac{1}{2\epsilon}\omega^2. \tag{3}$$

C. THE MODEL OF HIGH-SPEED TRAIN

Considering the train structure as show in Fig.1, we establish the model of HST consisting of a cascade of carriages, and carriages are connected by flexible couplers with each other.

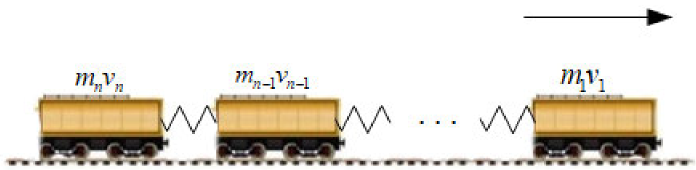

FIGURE 1. The Structure of high-speed Train.

The running resistance of each carriage satisfies:

$$R = c_0 + c_1 v + c_2 v^2, \tag{4}$$

where c_0, c_1 and $c_2 > 0$ denote the Davis' coefficients [32], which decided by the type of HST. When the train is moving, the performance of the couplers is described by the spring model as follow:

$$f(\Delta x) = k\Delta x, \tag{5}$$

where Δx denotes the relative spring displacement between two connected carriages and $k > 0$ is the elasticity coefficient of flexible couplers.

By applying Newton's second law into each carriage in Fig. 1, the dynamic of the HST with n carriages is established:

$$\begin{cases} \dot{x}_i(t) = v_i, i = 1, \ldots, n, \\ m_1\dot{v}_1(t) = u_1 - k(x_1 - x_2 - l) \\ \qquad - \left(c_0 + c_1 v_1 + c_2 v_1^2\right) m_1, \\ m_i \dot{v}_i(t) = u_i + k(x_{i-1} - x_i - l) - k(x_i - x_{i+1} - l) \\ \qquad - \left(c_0 + c_1 v_i + c_2 v_i^2\right) m_i, i = 2, \ldots, n-1, \\ m_n \dot{v}_n(t) = u_n + k(x_{n-1} - x_n - l) \\ \qquad - \left(c_0 + c_1 v_n + c_2 v_n^2\right) m_n, \end{cases} \tag{6}$$

where x_i and m_i are the ith carriage's position and mass, respectively, and l denotes the original length of the spring.

Assume the velocity at the equilibrium state satisfies $\overline{v}_1 = \overline{v}_2 = \ldots = \overline{v}_n = v_r$, and the distance between two connected cars satisfies $\overline{x}_{i-1} - \overline{x}_i = l$. Then the control force in the equilibrium state can be obtained:

$$\overline{u}_i = c_0 m_i + c_1 m_i v_r + c_2 m_i v_r^2. \tag{7}$$

Let $\tilde{x}_i(t) = x_i(t) - \bar{x}_i(t)$, $\tilde{v}_i(t) = v_i(t) - v_r$. According to (1) and (2), the following error systems can be obtained:

$$\begin{cases} \dot{\tilde{x}}_i(t) = \tilde{v}_i(t), \\ \dot{\tilde{v}}_i(t) = \dfrac{\tilde{u}_i(t)}{m_i} + \dfrac{k}{m_i} \sum_{j \in N_i^J} (\tilde{x}_j - \tilde{x}_i) - 2c_2 v_r \tilde{v}_i - c_1 \tilde{v}_i, \end{cases} \tag{8}$$

where N_i^J denotes the set of carriages connected with the ith carriage by flexible couplers.

III. MAIN RESULTS

This section contains three subsections. Section III-A introduces the proposed event-triggered control protocol of HST. In Section III-B, the avoidance of Zeno behavior is successful demonstrated in our system. Section III-C studies the active fault-tolerant control strategy of the HST under event-triggering.

A. EVENT-TRIGGERED CONSENSUS CONTROL FOR HSTs

Because of the large number of carriages on a single train, the burden of network transmission will be aggravated by the continuous communication. To overcome this defect, an event-triggered control protocol for the single high-speed train is proposed in this section.

For convenience, let $\left\{t_0^i, t_1^i, \ldots, t_k^i, \ldots\right\}$ denotes the sequence of triggering instants for the ith carriage. We assume that the tasks that need to be completed for each carriage i are as follows:

1) Receives the leader's information if $b_i > 0$. Receives its neighbors' latest transmitted status information $\tilde{x}_j\left(t_{k'}^j\right)$, $\tilde{v}_j\left(t_{k'}^j\right)$.

2) Continuously detects its own status information, and processes the received data according to the event-triggering function.

3) When the event-triggering function is satisfied, update its own controller and broadcast its status information of the latest triggering instant to its neighbors immediately.

Therefore, during $t \in \left(t_k^i, t_{k+1}^i\right)$, the event-triggered controller for the ith carriage is designed as follow:

$$\begin{aligned} \tilde{u}_i(t) &= u_i(t) - \overline{u}_i(t) \\ &= -\alpha m_i b_i \left(v_i\left(t_k^i\right) - v_r\right) - \beta m_i b_i \left(x_i(t_k^i) - \bar{x}_i\left(t_k^i\right)\right) \\ &\quad -\alpha m_i \sum_{j \in N_i} \left(v_i\left(t_k^i\right) - v_j\left(t_{k'}^j\right)\right) \\ &\quad -\beta m_i \sum_{j \in N_i} \left(x_i\left(t_k^i\right) - x_j\left(t_{k'}^j\right) - (j-i)l\right) \\ &= -\alpha m_i b_i \left(\tilde{v}_i\left(t_k^i\right)\right) - \alpha m_i \sum_{j \in N_i} \left(\tilde{v}_i\left(t_k^i\right) - \tilde{v}_j\left(t_{k'}^j\right)\right) \\ &\quad -\beta m_i b_i \left(\tilde{x}_i\left(t_k^i\right)\right) - \beta m_i \sum_{j \in N_i} \left(\tilde{x}_i\left(t_k^i\right) - \tilde{x}_j\left(t_{k'}^j\right)\right), \end{aligned} \tag{9}$$

where $b_i > 0$, if the ith carriage can receive its own target state from the leader; otherwise, $b_i = 0$. N_i denotes the neighboring set of the ith carriage, $t_{k'}^j$ is the lasted triggering instant of the jth carriage before t_k^i. The gain constant α, β are positive constants to be determined in sequel.

According to (9), the control $u_i(t)$ of each carriage i is composed of $\tilde{u}_i(t)$ and $\overline{u}_i(t)$. $\overline{u}_i(t)$ defined by (7) is used to

offset the running resistance during the operation of the train. And $\tilde{u}_i(t)$ is calculated from the state information of the leader and neighbors based on the communication topology. This part is used to make each carriage reach the target driving state.

By denoting the measurement errors of the ith carriage as $e_i^x(t) = x_i\left(t_k^i\right) - x_i(t)$, $e_i^v(t) = v_i\left(t_k^i\right) - v_i(t)$, the system (8) can be written as:

$$\begin{cases} \dot{\tilde{x}}_i(t) = \tilde{v}_i(t), \\ \dot{\tilde{v}}_i(t) = -\left[\alpha b_i\left(e_i^v(t) + \tilde{v}_i(t)\right) + \beta b_i\left(e_i^v(t) + \tilde{x}_i(t)\right)\right. \\ \quad + \alpha \sum_{j\in N_i}\left(\tilde{v}_i(t) - \tilde{v}_j(t) + e_i^v(t) - e_j^v(t)\right) \\ \quad \left. + \beta \sum_{j\in N_i}\left(\tilde{x}_i(t) - \tilde{x}_j(t) + e_i^x(t) - e_j^x(t)\right)\right] \\ \quad - \dfrac{k}{m_i}\sum_{j\in N_i^J}\left(\tilde{x}_i(t) - \tilde{x}_j(t)\right) - 2c_2 v_r \tilde{v}_i(t) \\ \quad - c_1\tilde{v}_i(t). \end{cases} \tag{10}$$

Let $\tilde{x}(t) = (\tilde{x}_1(t), \ldots, \tilde{x}_n(t))^T$, $\tilde{v}(t) = (\tilde{v}_1(t), \ldots, \tilde{v}_n(t))^T$, $e^x(t) = \left(e_1^x(t), \ldots, e_n^x(t)\right)^T$, $e^v(t) = \left(e_1^v(t), \ldots, e_n^v(t)\right)^T$. Then the above system (10) can be rewritten as follows:

$$\begin{cases} \dot{\tilde{x}}(t) = \tilde{v}(t), \\ \dot{\tilde{v}}(t) = -(\beta H + KJ)\tilde{x} \\ \quad -(\alpha H + (2c_2 v_r + c_1)I_N)\tilde{v} \\ \quad -\beta H e^x - \alpha H e^v, \end{cases} \tag{11}$$

where

$$J = \begin{bmatrix} 1 & -1 & 0 & \cdots & 0 \\ -1 & 2 & -1 & \ddots & \vdots \\ 0 & \ddots & \ddots & \ddots & 0 \\ \vdots & \ddots & -1 & 2 & -1 \\ 0 & \cdots & 0 & -1 & 1 \end{bmatrix},$$

$$K = \mathrm{diag}\{\frac{k}{m_1}, \frac{k}{m_2}, \cdots, \frac{k}{m_n}\},$$

$B = \mathrm{diag}\{b_1, b_2, \ldots, b_n\}$ is the leader adjacency matrix, and $H = \mathcal{L} + B$.

Let $\tilde{y}(t) = (\tilde{x}(t), \tilde{v}(t))^T$, $e_v^x(t) = (e^x(t), e^v(t))^T$, then system (11) can be further abbreviated as follow:

$$\dot{\tilde{y}}(t) = E\tilde{y}(t) + F e_v^x(t), \tag{12}$$

where

$$E = \begin{bmatrix} 0_{n\times n} & I_n \\ -(\beta H + KJ) & -(\alpha H + (2c_2 v_r + c_1)I_n) \end{bmatrix},$$
$$F = \begin{bmatrix} 0_{n\times n} & 0_{n\times n} \\ -\beta H & -\alpha H \end{bmatrix}.$$

Based on the second-order system (12), event-triggering function for the ith carriage is defined as follows:

$$f_i(t) = \xi_i\left(\|e_i^x\|^2 + \|e_i^v\|^2\right) - \eta_i\left(\|\tilde{x}_i\|^2 + \|\tilde{v}_i\|^2\right). \tag{13}$$

With $\xi_i = \frac{1}{2\epsilon}(\alpha + \beta)\|H\|$, $\eta_i = \sigma_i(\alpha\lambda_{\min}(H) + 2c_2 v_r + c_1 - 1 - \frac{\epsilon}{2}(\alpha + \beta)\|H\|)$, where $\epsilon > 0$, $\sigma_i \in (0, 1)$ is to be determined in sequel. When $f_i(t)$ reaches to zero, the ith carriage will be triggered. The measurement error is set to zero and will grow until the event-triggering function overpasses zero again.

Remark 1: For the convenience of research, this paper assumes that the control strategy is carried out in a fixed communication topology environment, that is, the value of H is fixed and known. However, it has some limitations. Further consideration of the control strategy under the condition of topology switching is a feasible research direction in the future.

Remark 2: Existing event triggering protocols in [27]–[29] used continuous information $x_j(t)$, $v_j(t)$ in their triggering functions. This type of event triggering scheme requires continuous communication between agents. Compared with continuous control, it can only save the calculation cost of the controller, and can not save the communication cost at all. There are also articles [33] that use $x_j\left(t_k^j\right)$, $v_j\left(t_k^j\right)$ in the triggering function, that is, they only need to communicate when the neighboring agents trigger, which can reduce the communication cost to a certain extent. However, compared with these articles, only own state information is needed in (13) for each carriage. Therefore, the communication burden can be further reduced.

B. STABILITY ANALYSIS OF THE CONSENSUS CONTROL SYSTEM

Based on the control protocol (9), we now study the criteria to guarantee the consensus of HST.

Theorem 1: Consider the single second-order high-speed train system with n carriages in (6). Assume the communication topology H contains a directed spanning, which means there exists at least one carriage can receive the messages from leader. For any bounded initial condition $x_i(t_0)$, $v_i(t_0)$, if the following conditions are satisfied, then all carriages of the train can achieve the consensus and track the desired speed v_r under event-triggered rule (13) and the distributed control protocol (9):

$$\begin{cases} \alpha > \dfrac{1}{\lambda_{\min}(H)}, \\ \beta > \alpha + \dfrac{2c_2 v_r + c_1 - 1}{\lambda_{\min}(H)}, \\ 0 < \epsilon < \dfrac{2\left(\alpha\lambda_{\min}(H) + 2c_2 v_r + c_1 - 1\right)}{(\alpha + \beta)\|H\|}, \\ 0 < \sigma_i < 1. \end{cases} \tag{14}$$

Proof 1: Consider the following Lyapunov function:

$$V(t) = \frac{1}{2}\tilde{y}(t)^T P\tilde{y}(t), \tag{15}$$

where $P = \begin{bmatrix} (\beta H + KJ) + \alpha H + (2c_2 v_r + c_1)I_n & I_n \\ I_n & I_n \end{bmatrix}$. From Lemma 1, we know that $H > 0$. Combining the definitions of other parameters, it is easy to guarantee that $(\beta H + KJ) + \alpha H + (2c_2 v_r + c_1)I_n > 0$. Then according to condition 2 in Lemma 2 and $\alpha > \frac{1}{\lambda_{\min}(H)}$ in (14), $P > 0$ can

be proved. Thus it can derive that $V(t)$ is positive definite. Expand the Lyapunov function as follows:

$$\begin{aligned} V(t) &= \frac{1}{2}\tilde{y}^T(t)P\tilde{y}(t) \\ &= \frac{1}{2}\tilde{x}^T\left[(\alpha+\beta)H + KJ + (2c_2v_r + c_1)I_n\right]\tilde{x} \\ &\quad +\tilde{x}^T\tilde{v} + \frac{1}{2}\tilde{v}^T\tilde{v}. \end{aligned} \tag{16}$$

Differentiating $V(t)$ along the trajectory (11) yields:

$$\begin{aligned} \dot{V} &= \tilde{x}^T\left[(\alpha+\beta)H + KJ + (2c_2v_r+c_1)I_n\right]\tilde{v} \\ &\quad +\tilde{v}^T\tilde{v} + \tilde{x}^T\dot{\tilde{v}} + \tilde{v}^T\dot{\tilde{v}} \\ &= \tilde{x}^T\left[(\alpha+\beta)H + KJ + (2c_2v_r+c_1)I_n\right]\tilde{v} \\ &\quad +\tilde{v}^T\tilde{v} - (\tilde{x}^T + \tilde{v}^T)\big[(\beta H + KJ)\tilde{x} + (\alpha H \\ &\quad +(2c_2v_r+c_1)I_n)\tilde{v} + \beta He^x + \alpha He^v\big] \\ &= -\tilde{x}^T(\beta H + KJ)\tilde{x} + (1 - 2c_2v_r - c_1)\tilde{v}^T\tilde{v} \\ &\quad -\alpha\tilde{v}^T H\tilde{v} - (\tilde{x}^T + \tilde{v}^T)(\beta He^x + \alpha He^v) \\ &\le -(\beta\lambda_{\min}(H) + \frac{k\lambda_{\min}(D)}{m_{\max}})\|\tilde{x}\|^2 + (1 - 2c_2v_r - c_1 \\ &\quad -\alpha\lambda_{\min}(H))\|\tilde{v}\|^2 - (\tilde{x}^T + \tilde{v}^T)(\beta He^x + \alpha He^v) \\ &\le -(\beta\lambda_{\min}(H))\|\tilde{x}\|^2 + (1 - 2c_2v_r - c_1 - \alpha\lambda_{\min}(H))\|\tilde{v}\|^2 \\ &\quad -\tilde{y}^T\begin{bmatrix}\beta H & \alpha H \\ \beta H & \alpha H\end{bmatrix}e_v^x \\ &\le -(\beta\lambda_{\min}(H))\|\tilde{x}\|^2 + (1 - 2c_2v_r - c_1 - \alpha\lambda_{\min}(H))\|\tilde{v}\|^2 \\ &\quad +(\alpha+\beta)\|H\|\|\tilde{y}\|\left\|e_v^x\right\|. \end{aligned} \tag{17}$$

From Lemma 3, one can obtain that:

$$\begin{aligned} (\alpha+\beta)\|H\|\|\tilde{y}\|\left\|e_v^x\right\| &\le \frac{\epsilon}{2}(\alpha+\beta)\|H\|\|\tilde{y}\|^2 \\ &\quad +\frac{1}{2\epsilon}(\alpha+\beta)\|H\|\left\|e_v^x\right\|^2. \end{aligned} \tag{18}$$

And it follows from (17) that:

$$\begin{aligned} \dot{V} &\le \sum_{i=1}^{n}\left[\left(-\beta\lambda_{\min}(H) + \frac{\epsilon}{2}(\alpha+\beta)\|H\|\right)\|\tilde{x}_i\|^2\right] \\ &\quad +\sum_{i=1}^{n}\Big[(-\alpha\lambda_{\min}(H) - 2c_2v_r - c_1 + 1 \\ &\quad +\frac{\epsilon}{2}(\alpha+\beta)\|H\|)\|\tilde{v}_i\|^2\Big] \\ &\quad +\sum_{i=1}^{n}\frac{1}{2\epsilon}(\alpha+\beta)\|H\|\left(\left\|e_i^x\right\|^2 + \left\|e_i^v\right\|^2\right). \end{aligned} \tag{19}$$

According to $\beta > \alpha + \frac{2c_2v_r + c_1 - 1}{\lambda_{\min}(H)}$ in (14), one can obtain that:

$$\begin{aligned} \dot{V} &\le \sum_{i=1}^{n}\Big[(-\alpha\lambda_{\min}(H) - 2c_2v_r - c_1 + 1 \\ &\quad +\frac{\epsilon}{2}(\alpha+\beta)\|H\|)\left(\|\tilde{x}_i\|^2 + \|\tilde{v}_i\|^2\right) \\ &\quad +\frac{1}{2\epsilon}(\alpha+\beta)\|H\|\left(\left\|e_i^x\right\|^2 + \left\|e_i^v\right\|^2\right)\Big]. \end{aligned} \tag{20}$$

From the event-triggering function (13), it is easy to guarantee that:

$$\xi_i\left(\left\|e_i^x\right\|^2 + \left\|e_i^v\right\|^2\right) \le \eta_i\left(\|\tilde{x}_i\|^2 + \|\tilde{v}_i\|^2\right). \tag{21}$$

Combining the definition of ξ_i, η_i, σ_i, we can derive that:

$$\begin{aligned} \dot{V} &\le \sum_{i=1}^{n}(\sigma_i - 1)\,(\alpha\lambda_{\min}(H) + 2c_2v_r + c_1 \\ &\qquad -\frac{\epsilon}{2}(\alpha+\beta)\|H\|)\,(\|\tilde{x}_i\|^2 + \|\tilde{v}_i\|^2). \end{aligned} \tag{22}$$

Thus, it can easily derive that $\dot{V}(t) < 0$ under the condition $0 < \epsilon < \frac{2(\alpha\lambda_{\min}(H) + 2c_2v_r + c_1 - 1)}{(\alpha+\beta)\|H\|}$ in (14). It comes to the conclusion that if conditions proposed above are satisfied, all carriages of the train can achieve the consensus and track the desired speed v_r under the distributed control protocol (9) and event-triggered rule (13).

For the reason introduced in Section 1, we need to avoid Zeno behavior in the design process in order to ensure the event-triggered strategy working successfully. Therefore, we are now in a position to proof the avoidance of Zeno behavior in Theorem 1 by following theorem.

Theorem 2: Under the consensus criterion we proposed in Theorem 1, the Zeno behavior doesn't exist in the error dynamical system (10) under the event triggered strategy (13), which means for any carriage i, the trigger interval time $\Delta_k^i = t_{k+1}^i - t_k^i > 0$.

Proof 2: Let $e_{\Delta ij} = \tilde{y}_j(t_k^i) - \tilde{y}_j(t_{k*}^j)$, where t_{k*}^j denotes the lasted triggering instant of carriage j before t. By defining e_Δ as $e_\Delta = (e_{\Delta i1}, e_{\Delta i2}, \ldots, e_{\Delta in})^T$, we can obtain that

$$\tilde{y}(t) = \tilde{y}(t_k^i) - e_\Delta - e_v^x(t).$$

Taking the derivative of $e_v^x(t)$ with respect to t along the trajectory of the error system (12) yields:

$$\begin{aligned} \frac{d}{dt}\left\|e_v^x(t)\right\| &= \frac{d}{dt}\|\tilde{y}(t)\| \\ &\le \|E\|\|\tilde{y}(t)\| + \|F\|\left\|e_v^x(t)\right\| \\ &\le \|E\|\left(\left\|\tilde{y}(t_k^i)\right\| + \|e_\Delta\|\right) \\ &\quad + (\|F\| + \|E\|)\left\|e_v^x(t)\right\|. \end{aligned} \tag{23}$$

Thus, we can derive the general solution of differential equation (23):

$$e_v^x(t) \le \frac{e^{(\|E\|+\|F\|)(t+C)} - \|E\|\left(\left\|\tilde{y}(t_k^i)\right\| + \|e_\Delta\|\right)}{(\|E\| + \|F\|)}. \tag{24}$$

Since $\left(\left|e_i^x(t)\right| + \left|e_i^v(t)\right|\right)$ is the ith element of vector $\left|\begin{bmatrix} I_n & I_n\end{bmatrix}\right|\left|e_v^x(t)\right|$, one can be obtained as follow:

$$\begin{aligned} &\left(\left\|e_i^x(t)\right\|^2 + \left\|e_i^v(t)\right\|^2\right) \\ &\quad \le \left\|\left|\begin{bmatrix} I_n & I_n\end{bmatrix}\right|\left|e_v^x(t)\right|\right\|^2 \\ &\quad \le 2\left\|e_v^x(t)\right\|^2 \\ &\quad \le 2\left[\frac{e^{(\|E\|+\|F\|)(t+C)} - \|E\|\left(\left\|\tilde{y}(t_k^i)\right\| + \|e_\Delta\|\right)}{(\|E\| + \|F\|)}\right]^2. \end{aligned} \tag{25}$$

With the fact that $\left\|e_i^x(t_k^i)\right\|^2 + \left\|e_i^v(t_k^i)\right\|^2 = 0$, one has:

$$C = \frac{\ln\left[\|E\|\left(\left\|\tilde{y}(t_k^i)\right\| + \|e_\Delta\|\right)\right]}{(\|E\| + \|F\|)}, \tag{26}$$

which means:

$$\left(\left\|e_i^x(t)\right\|^2 + \left\|e_i^v(t)\right\|^2\right) \le 2\left[Q\left(e^{(\|E\|+\|F\|)(t-t_k^i)} - 1\right)\right]^2, \tag{27}$$

where

$$Q = \frac{\|E\|\left(\left\|\tilde{y}(t_k^i)\right\| + \|e_\Delta\|\right)}{(\|E\| + \|F\|)}.$$

According to the event-trigger strategy (13), the next trigger time t_{k+1}^i of carriage i is determined by:

$$\left\|e_i^x(t_{k+1}^i)\right\|^2 + \left\|e_i^v(t_{k+1}^i)\right\|^2 = \frac{\eta_i\left(\left\|\tilde{x}_i(t_{k+1}^i)\right\|^2 + \left\|\tilde{v}_i(t_{k+1}^i)\right\|^2\right)}{\xi_i}.$$

When the system reaches stability, the system error is zero, and the control force of the system remains as (7). While before the system reaches stability, the system inevitably has errors, that is, $\|\tilde{x}_i\| + \|\tilde{v}_i\| > 0$. Then combining with (27) and $\xi_i, \eta_i > 0$, it can be verified that:

$$\begin{aligned} 0 &< \frac{\eta_i\left(\left\|\tilde{x}_i(t_{k+1}^i)\right\|^2 + \left\|\tilde{v}_i(t_{k+1}^i)\right\|^2\right)}{\xi_i} \\ &= \left\|e_i^x(t_{k+1}^i)\right\|^2 + \left\|e_i^v(t_{k+1}^i)\right\|^2 \\ &\le 2\left[Q\left(e^{(\|E\|+\|F\|)(t_{k+1}^i - t_k^i)} - 1\right)\right]^2. \end{aligned} \tag{28}$$

Now, Zeno behavior can be excluded for each carriage by contradiction. Assuming that there exists $\Delta_k^i = t_{k+1}^i - t_k^i \le 0$ for one of the carriages, then by the definition of Q, one can derive that $2\left[Q\left(e^{(\|E\|+\|F\|)(t_{k+1}^i - t_k^i)} - 1\right)\right]^2 \le 0$, which is violated with (28). Hence, no carriage of system (10) exhibits Zeno behavior during the consensus process under the event triggered strategy (13). The proof is completed.

C. EVENT-TRIGGERED CONSENSUS CONTROL UNDER ACTUATOR FAILURE

As a key system to ensure the smooth operation of the train, traction system plays an important role. However, the traction motor may experience fading actuation during long-term and high load operation. This kind of fault will affect the train operation performance. Therefore, this paper studies the requirement of fault estimation accuracy for systems with partial loss of actuator effectiveness. The actuator fault can be modelled as:

$$u_i^h = (1 - \rho_i)u_i^0(t), \tag{29}$$

where u_i^h denotes the actual actuator output of the ith carriage, and $u_i^0(t)$ denotes the designed actuator output of the ith carriage. The $\rho_i \in [0, 1)$ is a unknown time-varying value, reflecting the actuator fault severity of the ith carriage. When $\rho_i = 0$, the actuator is healthy, The case in which $0 < \rho_i < 1$ implies that the actuator of carriage i partially loses its actuating power (fading actuation) [34]. The fault severity increases with the increase of ρ_i.

Therefore, design the fault-tolerant control protocol as follows:

$$u_i^0(t) = (1 - \hat{\rho}_i)^{-1}u_i(t), \tag{30}$$

where $\hat{\rho}_i$ is the estimated value of ρ_i. According to [35], [36], $\hat{\rho}_i$ is assumed to be obtained by physical devices or technical analysis methods.

When the estimated value $\hat{\rho}_i$ is not precise, the control error can be calculated as:

$$\begin{aligned} u_i^f(t) &= u_i^h(t) - u_i(t) \\ &= \left[(1-\rho_i)(1-\hat{\rho}_i)^{-1} - 1\right]u_i(t) \\ &= -(\rho_i - \hat{\rho}_i)(1-\hat{\rho}_i)^{-1}u_i(t) \\ &= -\tilde{\rho}_i u_i(t), \end{aligned} \tag{31}$$

where $\tilde{\rho}_i = (\rho_i - \hat{\rho}_i)(1-\hat{\rho}_i)^{-1}$ and $u_i^h(t) = u_i^f(t) + u_i(t) = (1-\tilde{\rho}_i)u_i(t)$.

Combine with (6) and (7), we can further obtain the error dynamics system as follows:

$$\begin{cases} \dot{\tilde{x}}_i(t) = \tilde{v}_i(t), \\ \dot{\tilde{v}}_i(t) = \dfrac{1-\tilde{\rho}_i}{m_i}\tilde{u}_i(t) + \dfrac{k}{m_i}\sum\limits_{j\in N_i^J}(\tilde{x}_j - \tilde{x}_i) - 2c_2 v_r\tilde{v}_i - c_1\tilde{v}_i \\ \qquad -\tilde{\rho}_i(c_0 + c_1 v_r + c_2 v_r^2). \end{cases} \tag{32}$$

By using the same principle as subsection A, the system corresponding to (10) and (11) under active fault-tolerant control can be obtained as:

$$\begin{cases} \dot{\tilde{x}}_i(t) = \tilde{v}_i(t), \\ \dot{\tilde{v}}_i(t) = -(1-\tilde{\rho}_i)\big[\alpha b_i\left(e_i^v(t) + \tilde{v}_i(t)\right) + \beta b_i\left(e_i^v(t) + \tilde{x}_i(t)\right) \\ \qquad + \alpha\sum\limits_{j\in N_i}\left(\tilde{v}_i(t) - \tilde{v}_j(t) + e_i^v(t) - e_j^v(t)\right) \\ \qquad + \beta\sum\limits_{j\in N_i}\left(\tilde{x}_i(t) - \tilde{x}_j(t) + e_i^x(t) - e_j^x(t)\right)\big] \\ \qquad - \dfrac{k}{m_i}\sum\limits_{j\in N_i^J}\left(\tilde{x}_i(t) - \tilde{x}_j(t)\right) - 2c_2 v_r\tilde{v}_i(t) - c_1\tilde{v}_i(t) \\ \qquad - \tilde{\rho}_i(c_0 + c_1 v_r + c_2 v_r^2). \end{cases} \tag{33}$$

$$\begin{cases} \dot{\tilde{x}}(t) = \tilde{v}(t), \\ \dot{\tilde{v}}(t) = -[(I_n - \Delta)\beta H + KJ]\tilde{x} \\ \qquad -[(I_n - \Delta)\alpha H + (2c_2 v_r + c_1)I_n]\tilde{v} \\ \qquad -(I_n - \Delta)(\beta H e^x - \alpha H e^v) \\ \qquad -R(v_r)\tilde{\rho}. \end{cases} \tag{34}$$

where $\Delta = \mathrm{diag}\{\tilde{\rho}_1, \tilde{\rho}_2, \ldots, \tilde{\rho}_n\}$ and $\tilde{\rho} = (\tilde{\rho}_1, \tilde{\rho}_2, \ldots, \tilde{\rho}_n)^{\mathrm{T}}$. Based on the second-order system (34), event-triggering function for carriage i is defined as follows:

$$\begin{aligned} f_i(t) = \xi_i\left(\left\|e_i^x\right\|^2 + \left\|e_i^v\right\|^2\right) - \eta_i\left(\|\tilde{x}_i\|^2 + \|\tilde{v}_i\|^2\right) \\ + \frac{1}{\epsilon}R(v_r)|\tilde{\rho}_{\max}|^2, \end{aligned} \tag{35}$$

where $|\tilde{\rho}_{\max}| = \max\{|\tilde{\rho}_1|, |\tilde{\rho}_2|, \ldots, |\tilde{\rho}_n|\}$, and $\xi_i = \frac{1}{2\epsilon}(1+|\tilde{\rho}_{\max}|)(\alpha+\beta)\|H\|$,

$$\begin{aligned}\eta_i = \sigma_i\,(&\alpha\lambda_{\min}(H) + 2c_2 v_r + c_1 - 1\\ &- |\tilde{\rho}_{\max}|\,(\beta\lambda_{\max}(H) + \frac{1+\epsilon}{2}(\alpha+\beta)\|H\|)\\ &-\frac{\epsilon}{2}((\alpha+\beta)\|H\| + R(v_r))).\end{aligned}$$

Theorem 3: Consider the single second-order high-speed train system with actuator failure. Assume that the communication topology H contains a directed spanning, the distributed control protocol (30) is utilised and the event-triggering rule (35) is enforced. Then for any bounded initial condition $x_i(t_0)$, $v_i(t_0)$, all carriages of the train can achieve the consensus and track the desired speed v_r if the following conditions are satisfied:

Proof 3: Consider the same Lyapunov function as (15) and differentiating $V(t)$ along the trajectory (34) yields:

$$\begin{aligned}\dot{V} &= \tilde{x}^T\left[(\alpha+\beta)H + KJ + (2c_2v_r + c_1)I_n\right]\tilde{v}\\ &\quad + \tilde{v}^T\tilde{v} + \tilde{x}^T\dot{\tilde{v}} + \tilde{v}^T\dot{\tilde{v}}\\ &= \tilde{x}^T\left[(\alpha+\beta)H + KJ + (2c_2v_r + c_1)I_n\right]\tilde{v}\\ &\quad + \tilde{v}^T\tilde{v} - (\tilde{x}^T + \tilde{v}^T)\big[(\beta H + KJ)\tilde{x} + (\alpha H\\ &\quad + (2c_2v_r + c_1)I_n)\tilde{v} + \beta He^x + \alpha He^v\big]\\ &= -\tilde{x}^T(\beta H + KJ)\tilde{x} + (1 - 2c_2v_r - c_1)\tilde{v}^T\tilde{v}\\ &\quad -\alpha\tilde{v}^TH\tilde{v} - (\tilde{x}^T + \tilde{v}^T)(\beta He^x + \alpha He^v)\\ &\quad + (\tilde{x}^T + \tilde{v}^T)(\Delta\beta H\tilde{x} + \Delta\alpha H\tilde{v} + \Delta\beta He^x\\ &\quad + \Delta\alpha He^v - R(v_r)\tilde{\rho}).\end{aligned}\tag{37}$$

A separate analysis of the last item of (37) shows that:

$$\begin{aligned}A &= (\tilde{x}^T + \tilde{v}^T)(\Delta\beta H\tilde{x} + \Delta\alpha H\tilde{v} + \Delta\beta He^x\\ &\quad + \Delta\alpha He^v - R(v_r)\tilde{\rho})\\ &= \tilde{x}^T\Delta\beta H\tilde{x} + (\alpha+\beta)\tilde{x}^T\Delta H\tilde{v} + \tilde{v}^T\Delta\alpha H\tilde{v}\\ &\quad -(\tilde{x}^T + \tilde{v}^T)R(v_r)\tilde{\rho} + \tilde{x}^T\Delta\beta He^x\\ &\quad + \tilde{x}^T\Delta\alpha He^v + \tilde{v}^T\Delta\beta He^x + \tilde{v}^T\Delta\alpha He^v\\ &\leq \beta\,|\tilde{\rho}_{\max}|\,\lambda_{\max}(H)\|x\|^2 + (\alpha+\beta)\,|\tilde{\rho}_{\max}|\,\|H\|\,\|x\|\,\|v\|\\ &\quad + \alpha\,|\tilde{\rho}_{\max}|\,\lambda_{\max}(H)\|v\|^2 + R(v_r)\sum_{i=1}^{n}(|x_i\tilde{\rho}_i| + |v_i\tilde{\rho}_i|)\\ &\quad + y^T\begin{bmatrix}\Delta\beta H & \Delta\alpha H\\ \Delta\beta H & \Delta\alpha H\end{bmatrix}e_v^x.\end{aligned}\tag{38}$$

From Lemma 3, one can obtain that:

$$\begin{aligned}A &\leq \beta\,|\tilde{\rho}_{\max}|\,\lambda_{\max}(H)\|x\|^2 + \alpha\,|\tilde{\rho}_{\max}|\,\lambda_{\max}(H)\|v\|^2\\ &\quad + \frac{1}{2}(\alpha+\beta)|\tilde{\rho}_{\max}|\|H\|\|x\|^2 + \frac{1}{2}(\alpha+\beta)|\tilde{\rho}_{\max}|\|H\|\|v\|^2\\ &\quad + R(v_r)\sum_{i=1}^{n}(\frac{\epsilon}{2}\|x_i\|^2 + \frac{\epsilon}{2}\|v_i\|^2 + \frac{1}{\epsilon}\tilde{\rho}_i^2)\\ &\quad + \frac{\epsilon}{2}(\alpha+\beta)|\tilde{\rho}_{\max}|\|H\|\|y\|^2 + \frac{1}{2\epsilon}(\alpha+\beta)|\tilde{\rho}_{\max}|\|H\|\left\|e_v^x\right\|^2\\ &= [\beta\,|\tilde{\rho}_{\max}|\,\lambda_{\max}(H) + \frac{1}{2}(\alpha+\beta)\,|\tilde{\rho}_{\max}|\,\|H\| + \frac{\epsilon}{2}R(v_r)\\ &\quad + \frac{\epsilon}{2}(\alpha+\beta)\,|\tilde{\rho}_{\max}|\,\|H\|]\|x\|^2 + [\alpha\,|\tilde{\rho}_{\max}|\,\lambda_{\max}(H)\\ &\quad + \frac{1}{2}(\alpha+\beta)\,|\tilde{\rho}_{\max}|\,\|H\| + \frac{\epsilon}{2}R(v_r)\\ &\quad + \frac{\epsilon}{2}(\alpha+\beta)\,|\tilde{\rho}_{\max}|\,\|H\|]\|v\|^2 + \frac{R(v_r)}{\epsilon}\|\tilde{\rho}\|^2\\ &\quad + \frac{1}{2\epsilon}(\alpha+\beta)\,|\tilde{\rho}_{\max}|\,\|H\|\left\|e_v^x\right\|^2.\end{aligned}\tag{39}$$

And it follows from (37) that:

$$\begin{aligned}\dot{V} &\leq \sum_{i=1}^{n}[(-\alpha\lambda_{\min}(H) - 2c_2v_r - c_1 + 1\\ &\quad + \frac{\epsilon}{2}(\alpha+\beta)\,\|H\|)\left(\|\tilde{x}_i\|^2 + \|\tilde{v}_i\|^2\right)\\ &\quad + \frac{1}{2\epsilon}(\alpha+\beta)\,\|H\|\left(\left\|e_i^x\right\|^2 + \left\|e_i^v\right\|^2\right)] + A\\ &\leq \sum_{i=1}^{n}[(-\alpha\lambda_{\min}(H) - 2c_2v_r - c_1 + 1\\ &\quad + \frac{\epsilon}{2}(\alpha+\beta)\,\|H\| + \beta\,|\tilde{\rho}_{\max}|\,\lambda_{\max}(H)\\ &\quad + \frac{1}{2}(\alpha+\beta)\,|\tilde{\rho}_{\max}|\,\|H\| + \frac{\epsilon}{2}R(v_r)\\ &\quad + \frac{\epsilon}{2}(\alpha+\beta)\,|\tilde{\rho}_{\max}|\,\|H\|)\left(\|\tilde{x}_i\|^2 + \|\tilde{v}_i\|^2\right)\\ &\quad + \frac{1}{2\epsilon}(1+|\tilde{\rho}_{\max}|)(\alpha+\beta)\,\|H\|\left(\left\|e_i^x\right\|^2 + \left\|e_i^v\right\|^2\right)\\ &\quad + \frac{1}{\epsilon}R(v_r)\tilde{\rho}_i^2]\\ \dot{V} &\leq \sum_{i=1}^{n}[-(\alpha\lambda_{\min}(H) + 2c_2v_r + c_1 - 1\\ &\quad - |\tilde{\rho}_{\max}|\,(\beta\lambda_{\max}(H) + \frac{1+\epsilon}{2}(\alpha+\beta)\,\|H\|)\\ &\quad - \frac{\epsilon}{2}((\alpha+\beta)\,\|H\| + R(v_r)))\left(\|\tilde{x}_i\|^2 + \|\tilde{v}_i\|^2\right)\\ &\quad + \frac{1}{2\epsilon}(1+|\tilde{\rho}_{\max}|)(\alpha+\beta)\,\|H\|\left(\left\|e_i^x\right\|^2 + \left\|e_i^v\right\|^2\right)\\ &\quad + \frac{1}{\epsilon}R(v_r)\tilde{\rho}_{\max}^2].\end{aligned}\tag{40}$$

Combining the definition of ξ_i, η_i, σ_i, see (36) as shown at the bottom of the next page and the event-triggering function (35), it can derive that $\dot{V}(t) \leq 0$ for the similar reason as Theorem 1. It comes to the conclusion that all carriages of the train can achieve the consensus and track the desired speed v_r under the actuator failure and event-triggered rule if conditions proposed above are satisfied. The proof is completed.

IV. NUMERICAL RESULTS

In this section, two numerical examples are given to illustrate the effectiveness of the distributed event-triggered consensus control methods proposed by Theorems 1 and 2 under the second-order HST system. Case 3 is given to illustrate the effectiveness of the control methods proposed by Theorem 3 under time-varying actuator failure.

Case 1: In this example, the acceleration process of a HST consisting of 5 carriages is considered. Table 1 shows the

TABLE 1. Parameters of high-speed train.

Symble	Value	Unit
$m_i, i = 1, ..., 5$	40×10^3	kg
k	80×10^3	N/m
c_0	0.01176	N/kg
c_1	0.00077616	Ns/mkg
c_2	1.6×10^{-5}	Ns^2/m^2kg

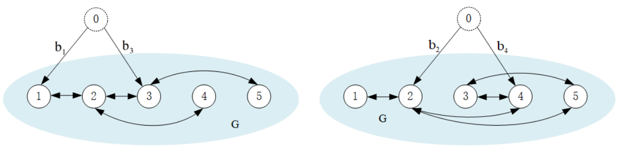

(a) Case 1.
(b) Case 2 and Case 3.

FIGURE 2. Communication topology of three Case.

system parameters of each carriage chosen from the experimental results of the Japan Shinkansen high speed train [37], and the simulation time is within 15 seconds.

In Fig. 2(a), the communication topology G is shown. The vertices of G are ordered from 1 to 5, and the solid lines describing the relationship of five carriages. It can be easily derived that there contains a directed spanning tree in the graph G. The vertex 0 denotes the virtual leader, which means the carriage 1 and 3 are pinned by the displacement feedback control.

Therefore, we can obtain that:

$$H = \begin{bmatrix} 2 & -1 & 0 & 0 & 0 \\ -1 & 3 & -1 & -1 & 0 \\ 0 & -1 & 3 & 0 & -1 \\ 0 & -1 & 0 & 1 & 0 \\ 0 & 0 & -1 & 0 & 1 \end{bmatrix}.$$

Considering that the most commonly used speed of high-speed train at present is about 230km/h, and the high-speed train with the speed over 300km/h is about to be put into operation. We did experiments in two velocity regions and compared them. In order to unify the units, we convert the speed units into m/s. Table 2 and Table 3 shows the initial position and speed of each carriage in two experiments. Suppose that the high-speed train expects

TABLE 2. The initial speeds and positions of each carriage(a).

i	1	2	3	4	5
$x_i(t_0)(m)$	10	7.6	5	3	0
$v_i(t_0)(m/s)$	60	61	60	59	60

TABLE 3. The initial speeds and positions of each carriage(b).

i	1	2	3	4	5
$x_i(t_0)(m)$	10	7.6	5	3	0
$v_i(t_0)(m/s)$	94	90	95	92	93

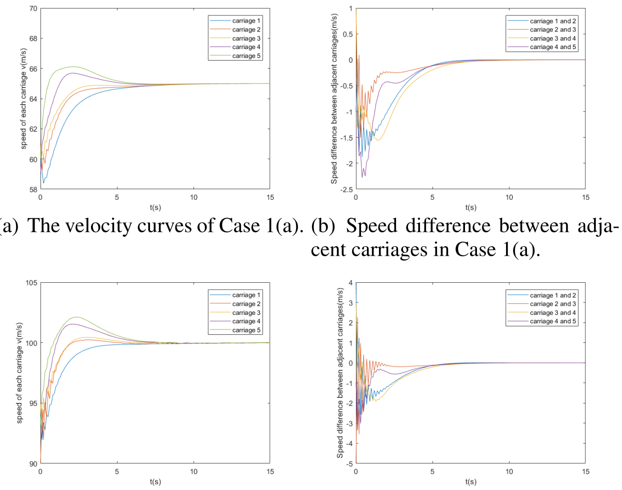

(a) The velocity curves of Case 1(a).
(b) Speed difference between adjacent carriages in Case 1(a).
(c) The velocity curves of Case 1(b).
(d) Speed difference between adjacent carriages in Case 1(b).

FIGURE 3. The velocity curves result of Case 1.

to increase its running speed to $v_r = 65m/s$ and $v_r = 100m/s$ and the distances between two neighbouring cars is about 1.5m. According to (14), choose coefficients $\alpha = 4, \beta = 1.3, \epsilon = 0.01$ and $\sigma_i = 0.98$. Thus, under the distributed control protocol (9) and event-triggered rule (13), the running speed curves of all carriages are shown in Fig. 3.

Fig. 3(a) and Fig. 3(c) show that all the carriages can quickly track the target speed under different initial conditions. Fig. 3(b) and Fig. 3(d) record the speed difference

$$\begin{cases} \alpha > \dfrac{1}{\lambda_{\min}(H)}, \\ \beta > \alpha + \dfrac{2c_2 v_r + c_1 - 1}{\lambda_{\min}(H)}, \\ 0 < \epsilon < \dfrac{2\left(\alpha\lambda_{\min}(H) + 2c_2 v_r + c_1 - 1\right) - 2\left|\tilde{\rho}_{\max}\right|\left[\beta\lambda_{\max}(H) + \frac{1}{2}(\alpha+\beta)\left\|H\right\|\right]}{(\alpha+\beta)\left\|H\right\| + \left|\tilde{\rho}_{\max}\right|\left[(\alpha+\beta)\left\|H\right\| - R(v_r)\right]}, \\ \left|\tilde{\rho}_{\max}\right| < \dfrac{\alpha\lambda_{\min}(H) + 2c_2 v_r + c_1 - 1}{\beta\lambda_{\max}(H) + \frac{1}{2}(\alpha+\beta)\left\|H\right\|}, \\ 0 < \sigma_i < 1. \end{cases} \tag{36}$$

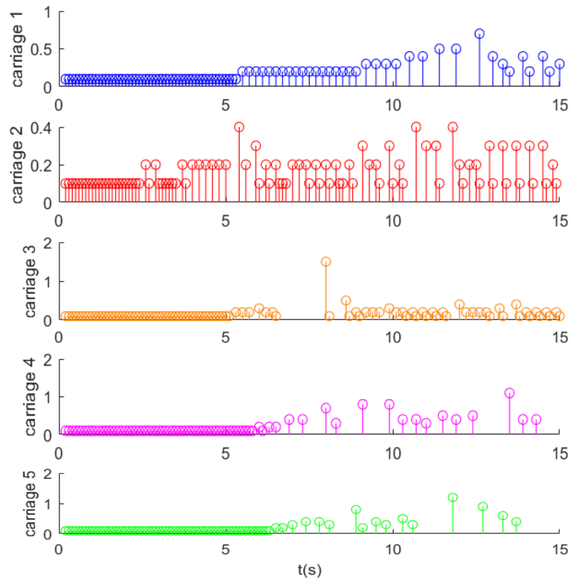

FIGURE 4. Trigger intervals of each carriages in Case 1.

between adjacent carriages in two experiment. It shows that in the lower speed case, the speed difference between adjacent carriages fluctuates within 2.5m/s, and finally reduces to 0. However, in the higher speed case, although the speed difference between adjacent carriages can be reduced to 0 finally, the fluctuation range before reaching stability is within 5m/s. Besides, Fig. 4 records the trigger intervals of five carriages for the higher speed experiment. From this figure we can see that the trigger frequency of each carriage slows down to varying degrees as the system gradually reaches consensus.

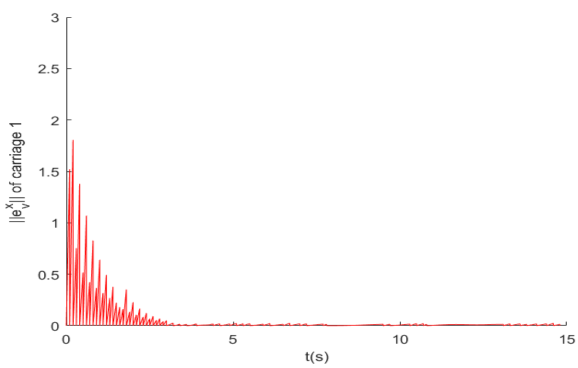

(a) carriage 1

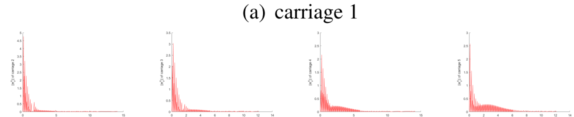

(b) carriage 2 (c) carriage 3 (d) carriage 4 (e) carriage 5

FIGURE 5. The measurement error of each carriage in Case 1.

At last, Fig. 5 shows the measurement error of each carriage in the control process. When the measurement error increases to a certain threshold, the carriage triggers, then the control is updated and the measurement error returns to zero.

TABLE 4. The initial speeds and positions of each carriage.

i	1	2	3	4	5
$x_i(t_0)(m)$	12	9	7.5	3	0
$v_i(t_0)(m/s)$	101	105	102	100	103

As the system stabilizes gradually, the threshold decreases with the system state error, and finally approaches zero.

Case 2: In this example, we consider the deceleration process of high-speed train with 5 carriages. The parameters of each carriage are the same with Case 1. Fig. 2(b) shows the communication topology of Case 2. Therefore, it can be obtained that:

$$H = \begin{bmatrix} 1 & -1 & 0 & 0 & 0 \\ -1 & 4 & 0 & -1 & -1 \\ 0 & 0 & 2 & -1 & -1 \\ 0 & -1 & -1 & 3 & 0 \\ 0 & -1 & -1 & 0 & 2 \end{bmatrix}.$$

Table 4 shows the initial position and speed of each carriage. Assume that the initial speed of each carriage is in the range of $100m/s$ to $105m/s$, the high-speed train expects to decrease its running speed to $v_r = 90m/s$ and the distances between two neighbouring cars is about 2m. According to (14), choose coefficients $\alpha = 3.3$, $\beta = 1$, $\epsilon = 0.002$ and $\sigma_i = 0.98$. Thus, under the event-triggered rule (13) and the distributed control protocol (9), the running speed curves of all carriages are shown in Fig. 6.

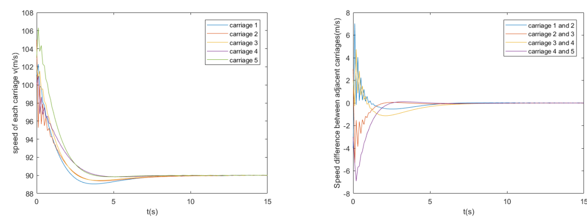

(a) The velocity curves of Case 2. (b) Speed difference between adjacent carriages in Case 2.

FIGURE 6. The velocity curves result of Case 2.

As Fig. 6 shows, all the carriages can track the desired speed under different initial conditions quickly. And the fluctuation range of speed difference between adjacent vehicles becomes larger due to the increase of speed. Moreover, Fig. 7 records the trigger intervals of five carriages. The same with Case 1, the trigger frequency of each carriage slows down to varying degrees as the system gradually reaches consensus. Finally, Fig. 8 shows the measurement error of each car in the control process.

According to these two cases, it is easy to see that different trains will have different trigger frequency changes in different communication topologies and initial states. But whether it is acceleration or deceleration, the high speed train can roughly track the target speed within 10 seconds. What's more, as the system tends to be stable, the trigger frequency

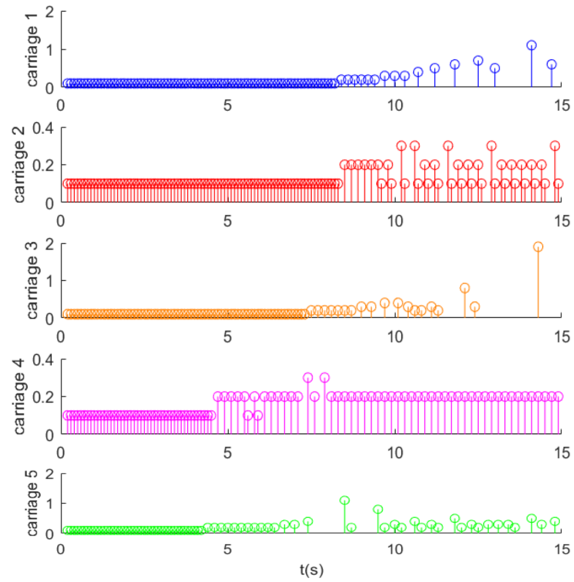

FIGURE 7. Trigger intervals of each carriages in Case 2.

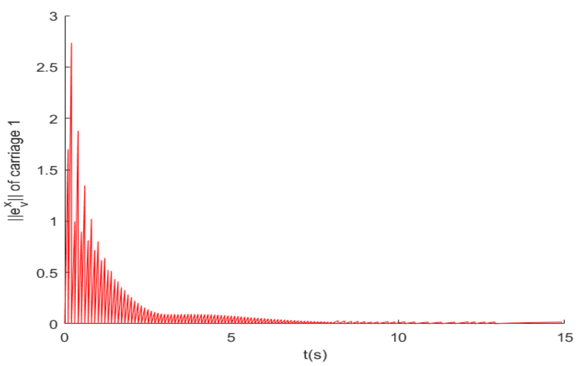

(a) carriage 1

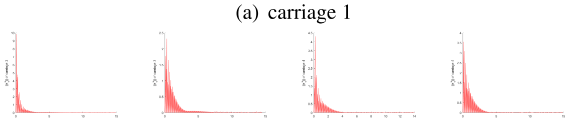

(b) carriage 2 (c) carriage 3 (d) carriage 4 (e) carriage 5

FIGURE 8. The measurement error of each carriage in Case 2.

of each carriage will slow down, thus can save computing and communication resources effectively.

Case 3: In this example, the same initial condition, target state and topology of 5 carriages as case 2 are considered. According to (36), we choose coefficients $\alpha = 3.3$, $\beta = 1$, $\epsilon = 0.0001$, $\sigma_i = 0.98$ and $|\tilde{\rho}_{\max}| = 0.15\%$. Thus, Fig. 9(a) shows the velocity curve of the Theorem 1 control scheme under time-varying actuator fault of carriages 3 and 4, where $\rho_3 = \rho_4 = 0.2*\sin(0.3t)+0.6$. Obviously, in the existence of the actuator failure, the system can never reach the consensus and event triggering has been maintained at a very frequent level.

Fig. 9(b) shows that when under the active fault-tolerant control designed in Theorem 3 and the accuracy of fault factor estimation by the fault detection system satisfies

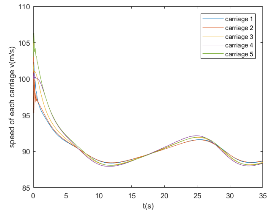

(a) The velocity curves without active fault tolerant control.

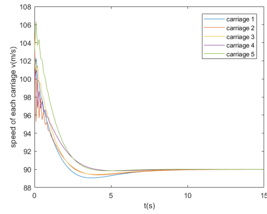

(b) The velocity curves under active fault tolerant control.

FIGURE 9. The velocity curves for each carriage in Case 3.

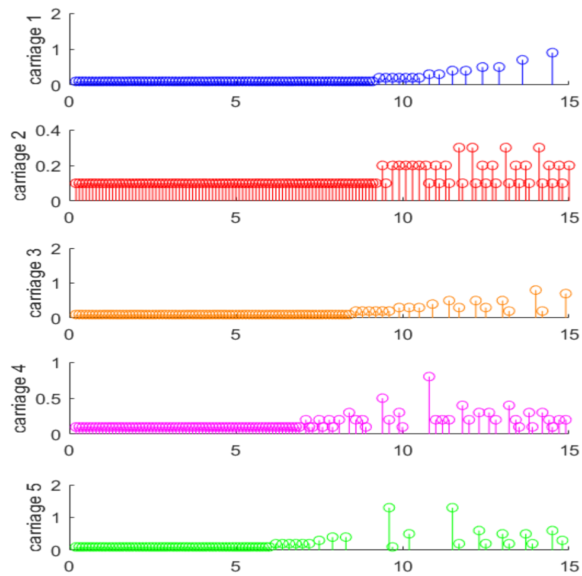

FIGURE 10. Trigger intervals of each carriages under the fault-tolerant control.

$|\tilde{\rho}_{\max}| = 0.15\%$, the speed variation curve of each carriage of high-speed train. Fig. 10 shows the trigger intervals of each carriages. Although the speed of tracking to the target state for each car is similar to that of the no-actuator fault under the fault-tolerant control(Compare Fig. 6(a) and Fig. 9(b)), the time and extent of the event trigger frequency reduction of each car in the fault condition still slightly worse than that in the case of no-actuator fault(Compare Fig. 7 and Fig. 10). Fig. 11 counts and compares the total trigger times of Case 2 and Case 3 within 15 seconds. Apparently, the trigger times under actuator fault is a little more than without fault. In general, the active fault-tolerant control proposed by Theorem 3 can resist the actuator failure mentioned well in this paper.

Remark 3: According to the statistical results in Fig. 11, although under the actuator fault, the average number of triggering times of each carriage within 15 seconds is less than 110, that is, the number of times that each compartment needs to calculate and update the controller is less than 110 within 15 seconds, and the average calculation interval is greater than 0.136 Seconds. Therefore, compared with continuous control, the event triggering strategy we used can effectively reduce the computational burden.

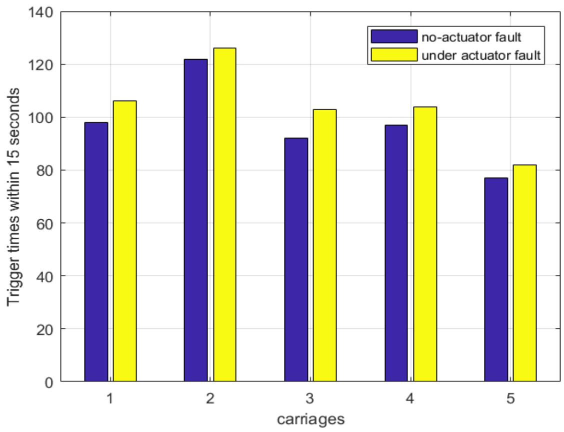

FIGURE 11. Statistical analysis of trigger times between Case 2 and Case 3.

V. CONCLUSION

The event-triggered consensus control strategy of the second-order high-speed train model under directed topology has been studied in this paper. To save unnecessary usage of communication and computing resources, the continuous communication among the neighbour carriages is unnecessary in the event-triggered control protocol we proposed. The criterion proposed in this paper has been of less conservatism compared with some existing results, and has proofed the avoidance of Zeno behavior. In addition, in order to enhance the reliability of the system, we also discusses the accuracy requirement of the fault diagnosis system when unknown time-varying actuator faults exist. Future research directions include the self-triggered sampling schemes, communication delay, etc.

REFERENCES

[1] C.-D. Yang and Y.-P. Sun, "Robust cruise control of high speed train with hardening/softening nonlinear coupler," in *Proc. Amer. Control Conf.*, vol. 3, Jun. 1999, pp. 2200–2204.

[2] H.-R. Dong, S.-G. Gao, B. Ning, and L. Li, "Extended fuzzy logic controller for high speed train," *Neural Comput. Appl.*, vol. 22, no. 2, pp. 321–328, Feb. 2013.

[3] H. Dong, B. Ning, B. Cai, and Z. Hou, "Automatic train control system development and simulation for high-speed railways," *IEEE Circuits Syst. Mag.*, vol. 10, no. 2, pp. 6–18, 2010.

[4] H. Zhao, X.-W. Dai, M. Zhang, and Q. Zhang, "An event-triggered robust cruise control strategy for multiple high-speed trains," in *Proc. Chin. Control Decis. Conf. (CCDC)*, Jun. 2018, pp. 2421–2426.

[5] X. Ge and Q.-L. Han, "Distributed formation control of networked multi-agent systems using a dynamic event-triggered communication mechanism," *IEEE Trans. Ind. Electron.*, vol. 64, no. 10, pp. 8118–8127, Oct. 2017.

[6] Y. Liu, F. Zhang, P. Huang, and Y. Lu, "Fixed-time consensus tracking for second-order multiagent systems under disturbance," *IEEE Trans. Syst., Man, Cybern. Syst.*, to be published.

[7] Y. Zhou, H. He, and C. Sun, "Fully distributed finite-time consensus of directed multiquadcopter systems via pinning control," *IEEE Trans. Syst., Man, Cybern. Syst.*, to be published.

[8] W. Ren and R. W. Beard, "Consensus algorithms for double-integrator dynamics," in *Distributed Consensus in Multi-Vehicle Cooperative Control: Theory and Applications*. London, U.K.: Springer, 2008, pp. 77–104.

[9] L. Ding and W. X. Zheng, "Network-based practical consensus of heterogeneous nonlinear multiagent systems," *IEEE Trans. Cybern.*, vol. 47, no. 8, pp. 1841–1851, Aug. 2017.

[10] W. He, G. Chen, Q.-L. Han, and F. Qian, "Network-based leader-following consensus of nonlinear multi-agent systems via distributed impulsive control," *Inf. Sci.*, vol. 380, pp. 145–158, Feb. 2017.

[11] W. He, B. Zhang, Q.-L. Han, F. Qian, J. Kurths, and J. Cao, "Leader-following consensus of nonlinear multiagent systems with stochastic sampling," *IEEE Trans. Cybern.*, vol. 47, no. 2, pp. 327–338, Feb. 2017.

[12] X.-M. Zhang and Q.-L. Han, "Network-based $\mathcal{H}_\infty$ filtering using a logic jumping-like trigger," *Automatica*, vol. 49, no. 5, pp. 1428–1435, May 2013.

[13] C. Peng, Q.-L. Han, and D. Yue, "To transmit or not to transmit: A discrete event-triggered communication scheme for networked Takagi–Sugeno fuzzy systems," *IEEE Trans. Fuzzy Syst.*, vol. 21, no. 1, pp. 164–170, Feb. 2013.

[14] X.-M. Zhang and Q.-L. Han, "A decentralized event-triggered dissipative control scheme for systems with multiple sensors to sample the system outputs," *IEEE Trans. Cybern.*, vol. 46, no. 12, pp. 2745–2757, Dec. 2016.

[15] P. Tabuada, "Event-triggered real-time scheduling of stabilizing control tasks," *IEEE Trans. Autom. Control*, vol. 52, no. 9, pp. 1680–1685, Sep. 2007.

[16] R. Pan, Y. Tan, D. Du, and S. Fei, "Adaptive event-triggered synchronization control for complex networks with quantization and cyber-attacks," *Neurocomputing*, vol. 382, pp. 249–258, Mar. 2020.

[17] M. Xiong, G. Ju, and Y. Tan, "Robust state estimation for fractional-order nonlinear uncertain systems via adaptive event-triggered communication scheme," *IEEE Access*, vol. 7, pp. 115002–115009, 2019.

[18] J. Liu, W. Suo, L. Zha, E. Tian, and X. Xie, "Security distributed state estimation for nonlinear networked systems against DoS attacks," *Int. J. Robust Nonlinear Control*, vol. 30, no. 3, pp. 1156–1180, Feb. 2020.

[19] J. Liu, M. Yang, X. Xie, C. Peng, and H. Yan, "Finite-time H_∞ filtering for state-dependent uncertain systems with event-triggered mechanism and multiple attacks," *IEEE Trans. Circuits Syst. I, Reg. Papers*, vol. 67, no. 3, pp. 1021–1034, Mar. 2020.

[20] J. Liu, M. Yang, E. Tian, J. Cao, and S. Fei, "Event-based security control for state-dependent uncertain systems under hybrid-attacks and its application to electronic circuits," *IEEE Trans. Circuits Syst. I, Reg. Papers*, vol. 66, no. 12, pp. 4817–4828, Dec. 2019.

[21] Y. Zhao and T. Wang, "Distributed control for high-speed trains movements," in *Proc. 29th Chin. Control Decis. Conf. (CCDC)*, May 2017, pp. 7591–7596.

[22] S. Li, L. Yang, K. Li, and Z. Gao, "Robust sampled-data cruise control scheduling of high speed train," *Transp. Res. C, Emerg. Technol.*, vol. 46, pp. 274–283, Sep. 2014.

[23] Y.-X. Li, "Finite time command filtered adaptive fault tolerant control for a class of uncertain nonlinear systems," *Automatica*, vol. 106, pp. 117–123, Aug. 2019.

[24] Y. Tan, S. Fei, J. Liu, and D. Zhang, "Asynchronous adaptive event-triggered tracking control for multi-agent systems with stochastic actuator faults," *Appl. Math. Comput.*, vol. 355, pp. 482–496, Aug. 2019.

[25] Y. Zhang and J. Jiang, "Bibliographical review on reconfigurable fault-tolerant control systems," *Annu. Rev. Control*, vol. 32, no. 2, pp. 229–252, Dec. 2008.

[26] L. Qin, X. He, and D. H. Zhou, "A survey of fault diagnosis for swarm systems," *Syst. Sci. Control Eng.*, vol. 2, no. 1, pp. 13–23, Dec. 2014.

[27] W. Zhu, Z.-P. Jiang, and G. Feng, "Event-based consensus of multi-agent systems with general linear models," *Automatica*, vol. 50, no. 2, pp. 552–558, Feb. 2014.

[28] H. Li, X. Liao, T. Huang, and W. Zhu, "Event-triggering sampling based leader-following consensus in second-order multi-agent systems," *IEEE Trans. Autom. Control*, vol. 60, no. 7, pp. 1998–2003, Jul. 2015.

[29] N. Huang, Z. Duan, G. Wen, and Y. Zhao, "Event-triggered consensus tracking of multi-agent systems with Lur'e nonlinear dynamics," *Int. J. Control*, vol. 89, no. 5, pp. 1025–1037, May 2016.

[30] J. Qin, W. X. Zheng, and H. Gao, "On pinning synchronisability of complex networks with arbitrary topological structure," *Int. J. Syst. Sci.*, vol. 42, no. 9, pp. 1559–1571, Sep. 2011.

[31] S. Boyd, L. El Ghaoui, E. Feron, and V. Balakrishnan, *Linear Matrix Inequalities in System and Control Theory*, vol. 15. Philadelphia, PA, USA: SIAM, 1994.

[32] W. J. Davis, *The Tractive Resistance of Electric Locomotives and Cars*. Boston, MA, USA: General Electric, 1926.

[33] M. Zhao, C. Peng, W. He, and Y. Song, "Event-triggered communication for leader-following consensus of second-order multiagent systems," *IEEE Trans. Cybern.*, vol. 48, no. 6, pp. 1888–1897, Jun. 2018.

[34] W. Cai, X. H. Liao, and Y. D. Song, "Indirect robust adaptive fault-tolerant control for attitude tracking of spacecraft," *J. Guid., Control, Dyn.*, vol. 31, no. 5, pp. 1456–1463, Sep. 2008.
[35] I. Saboori and K. Khorasani, "Actuator fault accommodation strategy for a team of multi-agent systems subject to switching topology," *Automatica*, vol. 62, pp. 200–207, Dec. 2015.
[36] K. Zhang, B. Jiang, and P. Shi, "Adjustable parameter-based distributed fault estimation observer design for multiagent systems with directed graphs," *IEEE Trans. Cybern.*, vol. 47, no. 2, pp. 306–314, Feb. 2016.
[37] T. Maeda, M. Kinoshita, H. Kajiyama, and K. Tanemoto, "Aerodynamic drag of shinkansen electric cars (series 0, series 200, series 100)," *Railway Tech. Res. Inst., Quart. Rep.*, vol. 30, no. 1, pp. 48–56, 1989.

WEIPING WANG received the Ph.D. degree in telecommunications physics electronics from the Beijing University of Posts and Telecommunications, Beijing, China, in 2015. She is currently an Associate Professor with the Department of Computer and Communication Engineering, University of Science and Technology Beijing. Her current research interests include auto-driving vehicle formation control, brain-like computing, memrisitive neural networks, associative memory awareness simulation, complex networks, network security, and image encryption. She received the National Key Research and Development Program of China, the State Scholarship Fund of China Scholarship Council, the National Natural Science Foundation of China, the Postdoctoral fund, and the basic scientific research project.

JINWEI LE received the B.Eng. degree from the University of Science and Technology Beijing, in 2018, where she is currently pursuing the master's degree. Her current research interests include auto-driving vehicle formation control, brain-like computing, and intelligent control.

ZHEN WANG received the Ph.D. degree from Hong 1287 Kong Baptist University, Hong Kong, in 2014. From 2014 to 2016, he was a JSPS Senior Researcher with the Interdisciplinary Graduate School of Engineering Sciences, Kyushu University, Fukuoka, Japan. Since 2017, he has been a Full Professor with Northwestern Polytechnical University, Xi'an, China. He has published more than 100 scientific articles, and his total citations are around 6,000 times and H-index is 40. His current research interests include complex networks, complex system, big data, evolutionary game theory, behavioral economic, and brain science. He was a recipient of the 1000 National Talent Plan Program of China.

XIONG LUO (Member, IEEE) received the Ph.D. degree in computer applied technology from Central South University, Changsha, China, in 2004. He is currently a Professor with the School of Computer and Communication Engineering, University of Science and Technology Beijing, Beijing, China. His current research interests include neural networks, machine learning, and computational intelligence. He has published extensively in his areas of interest in several journals, such as IEEE Access, *Future Generation Computer Systems*, and *Personal and Ubiquitous Computing*.

JÜRGEN KURTHS studied mathematics at the University of Rostock. He received the Ph.D. degree from the GDR Academy of Sciences, in 1983. He was a Full Professor with the University of Potsdam, from 1994 to 2008. He has been a Professor of nonlinear dynamics with Humboldt University, Berlin, and the Chair of the Research Domain Transdisciplinary Concepts of the Potsdam Institute for Climate Impact Research, since 2008, and the Sixth-Century Chair of Aberdeen University, U.K., since 2009. He has published more than 500 articles that are cited more than 18,000 times (H-factor: 57). His primary research interests include synchronization, complex networks, and time series analysis and their applications. He is a Fellow of the American Physical Society. He became a member of the Academia Europaea, in 2010, and of the Macedonian Academy of Sciences and Arts, in 2012. He received the Alexander von Humboldt Research Award from CSIR, India, in 2005, and an honorary doctorate from the Lobachevsky University Nizhny Novgorod and State University Saratov, in 2008 and 2012, respectively. He is an Editor of journals, such as *PLOS ONE, Philosophical Transaction of the Royal Society A, Journal of Nonlinear Science*, and *Chaos*.

MANMAN YUAN received the M.S. degree in computer science and technology from the Inner Mongolia University of Science and Technology, Baotou, China, in 2015. She is currently pursuing the Ph.D. degree with the University of Science and Technology Beijing, Beijing, China. Her current research interests include memristive neural networks and brain computing.

YOU MA received the Ph.D. degree from BUPT, in 2015. He is currently a Senior Engineer with the National Satellite Meteorological Center (NSMC), Beijing, China. His research interests include recommender systems, data mining, and deep learning.